Research article

Dev Reprod 2022;26(2):79-90
https://doi.org/10.12717/DR.2022.26.2.79

Development & Reproduction

ISSN 2465-9525 (Print)
ISSN 2465-9541 (Online)

Zebrafish Klf11b is Required to Maintain Cell Viability by Inhibiting p53-Mediated Apoptosis

†Hee Jeong Kong[1], Jung Jin Lee[2], Ju-Won Kim[1], Julan Kim[1], Young-Ok Kim[1], and †Sang-Yeob Yeo[2]

[1]*Biotechnology Research Division, National Institute of Fisheries Science, Busan 46083, Korea*
[2]*Dept. of Chemical and Biological Engineering, Hanbat National University, Daejeon 34158, Korea*

Received: March 18, 2022
Revised: April 24, 2022
Accepted: June 3, 2022

†Corresponding author
Hee Jeong Kong
Biotechnology Research Division, National Institute of Fisheries Science, Busan 46083, Korea.
Tel: +82-51-720-2455
Fax: +82-51-720-2456
E-mail: heejkong@korea.kr
Sang-Yeob Yeo
Department of Chemical and Biological Engineering, Hanbat National University, Daejeon 34158, Korea.
Tel: +82-42-821-1552
Fax: +82-42-821-1692
E-mail: yeosy@hanbat.ac.kr

ORCID
Hee Jeong Kong
https://orcid.org/0000-0001-6524-6544
Jung Jin Lee
https://orcid.org/0000-0002-6048-927X
Ju-Won Kim
https://orcid.org/0000-0002-4220-711X
Julan Kim
https://orcid.org/0000-0003-1964-9486
Young-Ok Kim
https://orcid.org/0000-0001-8719-0764
Sang-Yeob Yeo
https://orcid.org/0000-0002-1697-5641

Conflict of interests
The authors declare no potential conflict of interest.

Abstract

Krüppel-like factor 10 (KLF10) regulates various cellular functions, such as proliferation, differentiation and apoptosis, as well as the homeostasis of several types of tissue. In the present study, we attempted a loss-of-function analysis of zebrafish *Klf11a* and *Klf11b*, which constitute human KLF10 homologs. Embryos injected with *klf11b-morpholino* (*MO*) showed developmental retardation and cell death, whereas *klf11a-MO*-injected embryos showed normal development. In *klf11b-MO*-injected embryos, a dramatic increase in the amount of zebrafish *p53* mRNA might be the cause of the increase in that of *bax*. The degree of apoptosis decreased in the *klf11b-MO* and *p53-MO* co-injected embryos. These findings imply that KLF10 is a negative regulator of p53-dependent transcription, suggesting that the KLF10/p53 complex may play an important role in apoptosis for maintenance of tissue homeostasis during embryonic development.

Keywords: *Klf11b*, Krüppel-like factor 10 (KLF10), *p53*, Zebrafish

INTRODUCTION

Krüppel-like factors (KLFs) encode C2H2-type zinc finger proteins that regulate various cellular functions, such as proliferation, differentiation, and apoptosis in the development (Black et al., 2001; Subramaniam et al., 2010). In mammals, 14 KLF genes have been identified as transcription factors; these belong to the Sp1 superfamily (Black et al., 2001). Human KLF10 was initially isolated from fetal osteoblasts treated with tumor growth factor-β (TGF-β); thus, its original name was TGF-β-inducible gene 1 (TIEG1) (Subramaniam et al., 1995). Human KLF11 (originally termed TGF-β-inducible gene 2) was identified by BLAST using the EST database for rat TIEG sequences (Cook et al., 1998). Overexpression of either KLF10 or KLF11 caused inhibition of cell proliferation and induction of apoptosis (Subramaniam et al., 2010). Mouse KLF10 knockout (KO) caused an increase in the predisposition of epidermal tumorigenesis and development of epidermal inclusion cysts after 7,12-dimethylbenz(a)anthracene and 12-O-tetradecanoylphorbol-13-acetate (DMBA/TPA) treatment (Song et al., 2012). Although the increased number of BrdU-positive cells in KLF10 KO mice supports the hypothesis that cell proliferation is inhibited by human KLF10, the relation between tumorigenesis in KLF10 KO mice and apoptosis in human KLF10-overexpressing cells remains unclear. As KLF10

Acknowledgements
We thank the members of Yeo and Kong's Lab. This research was supported by a grant from the National Institute of Fisheries Science (NIFS), Korea (R2022027).

Authors' contributions
Conceptualization: Yeo SY.
Data curation: Kong HJ.
Formal analysis: Kim JW.
Methodology: Kong HJ, Lee JJ, Kim JW, Kim YO.
Writing-review & editing: Kong HJ, Yeo SY.

Ethics approval
The experiment was approved by the Institutional Animal Care and Use Committee (2015-NFRDI-IACUC-1)

KO mice exhibited a lower incidence of tumors during DEN-induced hepatic carcinogenesis (Heo et al., 2015), we suspect that a loss-of-function analysis in another model animal may aid understanding of the function of KLF10.

The Zebrafish Klf family is subdivided into four groups, consistent with the classification used for their mammalian homologs (Xue et al., 2015). Zebrafish Klf9, Klf10, Klf11a, Klf11b, Klf13, and Klf16 belong to members of group 4, which may facilitate transcriptional regulation by interacting with putative binding sites of Sin3A (Xue et al., 2015). Although a previous study showed that the respective losses of zebrafish Klf3 (group 3) and zebrafish Klf6a (group 2) led to an increased number of erythroid progenitor cells (EPC) and a smaller number of erythrocytes (Xue et al., 2015), these observations may be insufficient for a comprehensive analysis of the KLF family during embryogenesis in vertebrates. Moreover, they cannot provide new insights into the functions and mechanisms of KLF family during maintenance of cell homeostasis.

In the present study, we attempted a loss-of-function analysis of zebrafish homologs of human Klf10 by using antisense MO. Zebrafish *Klf11a* and *Klf11b* were isolated and characterized as homologs of human KLF10. Investigation of zebrafish *Klf11b* function in maintenance of cell homeostasis showed possible interactions between *klf11b* and *p53*. Our findings suggest that the relationship between *Klf11b* and *p53* may play an important role during embryonic development in zebrafish.

MATERIAL AND METHODS

1. Zebrafish maintenance

Zebrafish were maintained as described by Yeo et al. (2004). The embryos were staged in accordance with the method of Kimmel et al. (1995). AB* wild-type and *Tg[islet1:GFP]* (Higashijima et al., 2000) were used.

2. Isolation of cDNAs and RT-PCR

The sequences of zebrafish *klf11a* (NM001044941), *klf11b* (NM001077604), *EF1a* (NM131263), *p53* (U60804), *Bax* (BC055592), and *caspase 3* (NM131877) were identified in GenBank. Total RNA of *Con-MO*-, *klf11a-MO*-, and/or *klf11b-MO*-injected embryos were employed for RT-PCR. PCR was performed using the primers as described in Table 1. PCR products, so called cDNA, were subcloned into the pGEM-T vector, and then verified by sequencing.

3. Whole-mount *in situ* hybridization

Whole-mount *in situ* hybridization was performed as described by Yeo et al. (2004). Antisense riboprobes were transcribed from cDNAs for zebrafish *klf11a*, *klf11b*, *p53*, *Bax*, and *caspase-3*. Photos were taken with a differential interference contrast microscope (Axiopan2; Carl Zeiss, Oberkochen, Germany).

4. Confocal imaging and cell transplantation

Immunohistochemistry was performed as described by Yeo et al. (2004). Anti-phospho-histone H3 was used as the primary antibody (Upstate). AlexaFluor 568-conjugated goat anti-rabbit IgG was used as secondary antibody (Molecular Probes). Photos were taken with a confocal laser scanning microscope (LSM700; Carl Zeiss).

Cell transplantation was performed as described by Jung et al. (2012). Cells from *klf11b-MO*-

https://doi.org/10.12717/DR.2022.26.2.79

Table 1. Primer list

Primer name	Sequence
klf11b RT_F	5'-GGA GCT CGG ATG GAG GTC TGT-3'
klf11b RT_R	5'-ATT GCA GAC ATA GTT GCG CCT-3'
klf11a RT_F	5'-TGC GGA AAC TTC AGG CAC AGC GGT-3'
klf11a RT_R	5'-ATG AAA CGG CGC TCA CAG ACA GGA-3'
EF1a RT_F	5'-TAT CAC CAT TGA CAT TGC TCT-3'
EF1a RT_R	5'-CAT CTC CGG ATT TGA GAG CCT-3'
p53 RT_F	5'-GTG CAT GTC CAG GCA GAG ACA-3'
p53 RT_R	5'-TGC TGC TTA CAA AAC AAC CGA-3'
Bax RT_F	5'-GGA GTT ATC ACC ACA GCA TTG-3'
Bax RT_R	5'-CTG CTG CCA CGC CAC CTC ATA-3'
Cas3 RT_F	5'-ATG GTC GTG AAA GGA TCC CAG-3'
Cas3 RT_R	5'-TCT CCA ATC TCA CTG ATT TAA-3'

and fluorescein-dextran-injected embryos, as well as from *klf11a-MO*- and rhodamine-dextran-injected embryos, were used as donors. Cell transplants were performed at the mid-blastula stage. At 10 h after transplantation, embryos were fixed with 4% PFA and mounted using Vectashield with DAPI (Vector Labs). Confocal images were taken at the 15-somite stage with a confocal laser scanning microscope (LSM700; Carl Zeiss).

5. Morpholino (MO) injection

Microinjection was performed as described by Yeo et al. (2004). Spliced *klf11a-MO* (5'-TAG AGT CAC TCA CCA GTG ATG AGA G-3'; Gene Tools, Philmath, OR, USA), 4-bp mismatched *klf11a control-MO* (5'-TAG AGA CAC TGT CCA GTC ATG AGA G-3'; Gene Tools), spliced *klf11b-MO* (5'-GGT CAT GCA CTG CAG GTA AAC AGG A-3'; Gene Tools), 3-bp mismatched *klf11b control-MO* (5'-GGT CAA GCA CAC CAG GTA AAC AGG A-3'; Gene Tools), and *p53-MO* (5'-GCG CCA TTG CTT TGC AAG AAT TG-3'; Gene Tools) (2–4 ng) were injected into fertilized zebrafish eggs.

6. Northern blot

Total RNA was extracted from embryos at the 1-cell stage, as well as at 6-, 12-, and 24-hpf using TRIzol™ reagent (Invitrogen, Carlsbad, CA, USA). Their isolation was performed as described by manufacturer. Total RNA of *Con-MOs*-, *klf11a-MO*-, and/or *klf11b-MO*-injected embryos were used for Northern blot analyses. DIG-labelled zebrafish *klf11a*, *klf11b*, *EF1a*, *p53*, *Bax*, and *caspase-3* were used as probes. Anti-Dig secondary antibodies were detected with an ECL kit (KPL, Boca Raton, FL, USA).

7. TUNEL assay

The TUNEL assay was performed as described in Song et al. (2012). Zebrafish embryos injected with *Con-MOs* or *klf11b-MO* were fixed with 4% PFA overnight and then dehydrated with methanol. Apoptotic cells were detected using the *In Situ* Cell Death Detection Kit, in accordance with the manufacturer's instructions (Roche, Basel, Switzerland).

RESULTS

1. Expression of zebrafish *klf11a* and *klf11b*

Two zebrafish homologs of human KLF10 were identified and characterized *in silico* using GenBank and the Sanger zebrafish genome assembly (www.ensembl.org). The predicted amino acid (AA) sequence of human KLF10 had approximately 54% and 49% similarity to predicted sequences of zebrafish *Klf11b* and *Klf11a*, respectively, whereas the predicted sequence of human KLF11 had approximately 57% and 57% similarity to predicted sequences of zebrafish *Klf11a* and *Klf11b*, respectively. Therefore, zebrafish *Klf11a* was classified as a homolog of human KLF11, while zebrafish *Klf11b* was classified as a homolog of human KLF10.

To examine the spatial and temporal expression of zebrafish homologs of human KLF10/11, we performed whole-mount *in situ* hybridization using *klf11a* and *klf11b* genes at various stages (Fig. 1). A very low level of *klf11b* mRNA was detected ubiquitously in zebrafish embryos at the gastrula stage (data not shown). At 12 h post-fertilization (hpf), mRNA expression of *klf11b* was concentrated in the hindbrain primordia of the neural plate (Fig. 1A). This expression in the neural plate was maintained in the hindbrain at 24 hpf (Fig. 1B). At this stage, *klf11b* mRNA was highly expressed in the olfactory bulb, lens, and somites, while weaker expression levels were detected in the nervous system (Figs. 1B and C). Transcripts of *klf11b* were also present in the pronephric

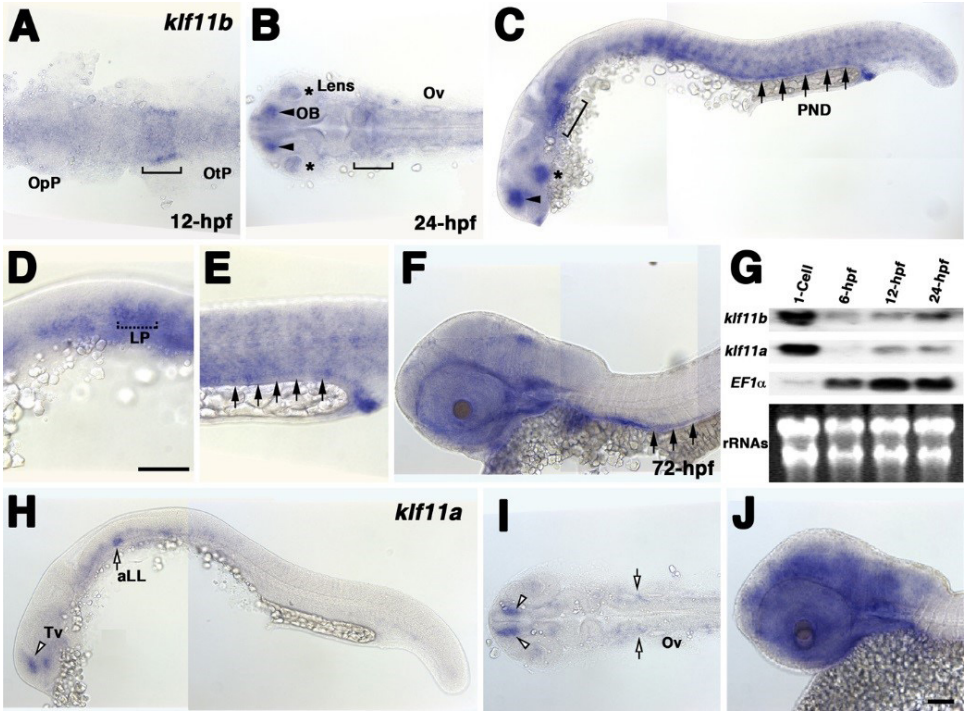

Fig. 1. Expression of zebrafish *klf11a* and *klf11b*. Dorsal views (A, B, and I), lateral views (C–F, H, and J), and anterior to the left. (A–F), Expression of *klf11b* mRNA at 12-h post-fertilization (hpf) (A), 24-hpf (B–E), and 72-hpf (F). Transcripts of *klf11b* are detected in the hindbrain (bracket), olfactory bulb (OB, arrowheads), lens (asterisks), lateral primordial cells (LP, dotted line), and pronephric ducts (PND, arrows). (G), Northern blot analysis for zebrafish *klf11a*, *klf11b*, and *elongation factor-1alpha* (*EF1α*) mRNA at different stages, as indicated (1-cell stage and 6–24 hpf). In total, 20 μg of total RNA from the embryo are applied to each lane. The bottom panel shows the corresponding 18S and 28S rRNA bands. (H–J), Expression of *klf11a* mRNA at 24-hpf (H, I) and 72-hpf (J). Transcripts of *klf11a* are detected in the ventral telencephalon (Tv, open arrowheads) and the anterior lateral line (aLL, open arrows). OpP, optic primordium; OtP, otic primordium; OV, otic vesicle. Scale bars, 100 μm (A–F, H–J).

https://doi.org/10.12717/DR.2022.26.2.79

duct (PND) and lateral primordia (Figs. 1C–E). At 72 hpf, transcripts of *klf11b* were consistently observed in the PND, with weaker expression levels seen in the nervous system (Fig. 1F). Northern blot analysis of zebrafish *klf11* homologs showed maternal expression of their transcripts (Fig. 1G). Although transcripts of *klf11a* were difficult to detect by whole-mount *in situ* hybridization until 12 hpf, Northern blot analysis showed that *klf11a* mRNA was present at low levels from 12 hpf through 24 hpf (Fig. 1G). In contrast to the relatively broad expression of *klf11b* at 24 hpf, *klf11a* was expressed in spatially restricted domains of telencephalon, as well as in the anterior lateral line at low levels (Figs. 1H and 1I). At 72 hpf, transcripts of *klf11a* were persistently observed in telencephalon, with strong expression in the nervous system (Fig. 1J).

2. Zebrafish *klf11b* morphant shows cell death

Our observation that transcripts of both *klf11a* and *klf11b* are maternally expressed suggested that they may be involved in control of early embryogenesis. As an initial step in analysis of the role of zebrafish homologs of human KLF10/11, we attempted to knock down *klf11a* and *klf11b* by injecting their MOs (ATG-MOs, which bind to a sequence on, or close to, the ATG start site of mRNA) into the embryos. A mixture of ATG-MOs caused severe developmental defects that interfered with analysis of morphological abnormalities after the gastrula stage (data not shown). Thus, we designed splice-site MOs to inhibit zygotic transcripts (Fig. 2). Reverse-transcription (RT)-PCR showed that embryos injected with 4 pg of *klf11b-MO* or *klf11a-MO* had abnormal amplicons of 1,728 base pairs (bp) or 1,721 bp at the 15-somite stage, respectively (Fig. 2A). Three bp-*klf11b mismatch-MO* was used as a control, and embryos injected with this MO did not generate alternate transcripts (Lane 3 in Fig. 2A). However, 4 bp-*klf11a mismatch-MO* slightly blocked pre-mRNA splicing of *klf11a* (Lane 2 in Fig. 2A). Abnormalities could be observed in embryos injected with a 4-pg mixture of *klf11b-MO* and *klf11a mismatch-MO* at the 15-somite stage, although these embryos developed normally through the end of gastrulation (Fig. 2C). By 16 hpf, all *klf11* morphants could be separated into one of two groups: (i) moderate, characterized by cell death in the retina (Figs. 2C–2E); or (ii) severe, characterized by cell death in retina, as well as somites (Figs. 3B and 3C). The morphant phenotype was 54% moderate and 46% severe (n=52, Fig. 3). Embryos injected with 4 pg of *klf11b mismatch-MO* and *klf11a mismatch-MO* (*Con-MOs*) (Fig. 2B, n=50), as well as those injected with *klf11a-MO* and *klf11b mismatch-MO* (Fig. 2D, n=51), developed normally until 16 hpf (Fig. 2, Fig. 3).

To assess whether Klf11a and Klf11b function in a cell-autonomous manner, we performed cell transplantation experiments (Figs. 2F–2I). At 3.5 hpf, cells from donor embryos that had been injected with *klf11b-MO* and FITC-dextran were mixed with cells from embryos that had been injected with *klf11a-MO* and rhodamine-dextran, and then transferred into wild-type embryos (Fig. 2I). At 16 hpf, *klf11a-MO*-injected cells were normally developed (Fig. 2F), whereas atypical nuclei were observed in the green channel (Figs. 2G–2H). This observation suggested that cells injected with *klf11b-MO* might undergo cell death, and that Klf11b functions in a cell-autonomous manner.

To assess embryos injected with *klf11b-MO*, we performed whole-mount *in situ* hybridization with *p53*, *Bax*, and *caspase-3*, all of which are involved in cell death in zebrafish (Fig. 4). Based on phenotypic analysis (Fig. 2C), embryos injected with *klf11b-MO* were fixed at the 5-somite stage (Figs. 4A–4F). Zebrafish *p53* was ubiquitously expressed in *Con-MO*-injected embryos (Fig. 4A). However, its transcripts were dramatically increased in *klf11b-MO*-injected embryos (Fig. 4B). Compared to control embryos (Fig. 4C), the expression of *bax*, a direct target of p53, also increased (Fig. 4D). These data were consistent with the hypothesis that overexpressed *Bax* accelerates apoptotic cell death and counters the death repressor activity of Bcl-2 (Oltval et al., 1993). The expression of *caspase-3* was examined at the 5-somite stage (Fig. 4E), which showed that

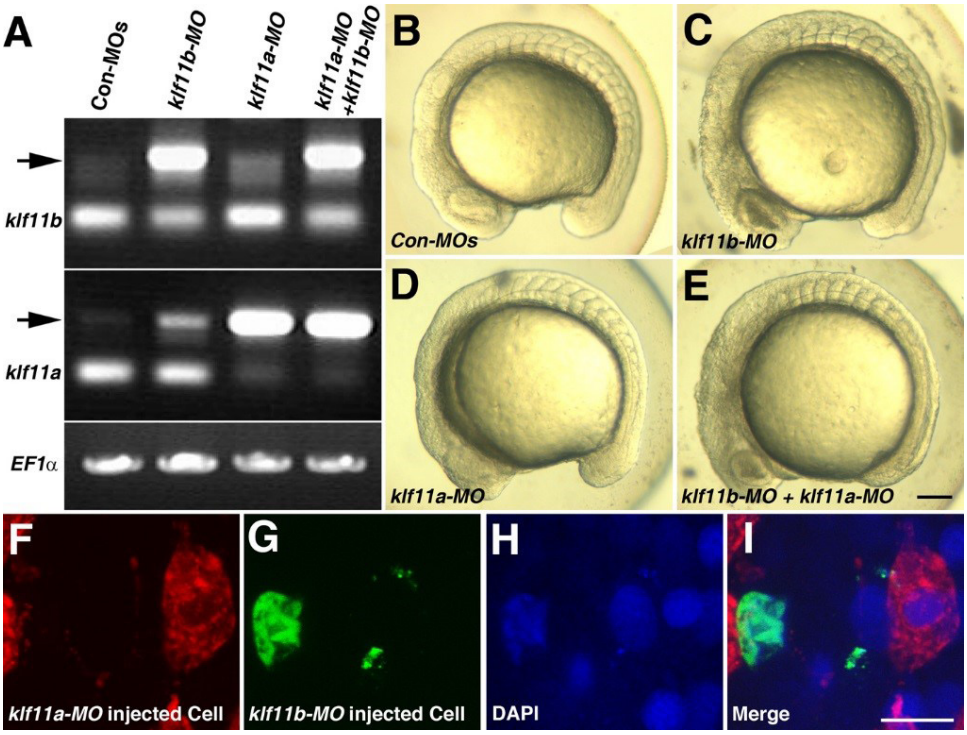

Fig. 2. Effects of zebrafish *klf11a* and *klf11b* morpholinos (MOs). (A), Reverse transcription-polymerase chain reaction (RT-PCR) analysis shows *klf11a* transcripts (981 bp), *klf11b* transcripts (996 bp), and *EF-1α* transcripts (986 bp) from embryos injected with corresponding splice MOs and control MOs (*Con-MOs*; *klf11a mismatch-MO* and *klf11b mismatch-MO*). Unspliced RNA of *klf11b* (1,728 bp) is detected in embryos injected with *klf11b-MO* and *klf11a mismatch-MO*, as well as those injected with *klf11a-MO* and *klf11b-MO* (arrow in upper panel). Unspliced RNA of *klf11a* (1,721 bp) is detected in embryos injected with *klf11a-MO* and *klf11b mismatch-MO*, as well as those injected with *klf11a-MO* and *klf11b-MO* (arrow in lower panel). (B–E), Phenotypic analysis of *klf11a* and *klf11b* morphants. Lateral views, anterior to the left. The mixture of *klf11a mismatch-MO* and *klf11b mismatch-MO* (*Con-MOs*) was injected into zebrafish eggs as a control (B, n=50). At the 15-somite stage, degenerative and developmental defects are observed in embryos injected with *klf11b-MO* and *klf11a mismatch-MO* (C, n=21), as well as in embryos injected with *klf11a-MO* and *klf11b-MO* (E, n=31), but not in embryos injected with *klf11a-MO* and *klf11b mismatch-MO* (D, n=51). (F–I), Cell transplantation analysis reveals the cell-autonomous function of Klf11b. Confocal images show a *klf11a-MO*- and rhodamine-dextran-injected cell in the red channel (F) and a *klf11b-MO*- and FITC-dextran-injected cell in the green channel (G). DAPI-stained genomic DNA is shown in the blue channel (H) and the merge image is displayed (I). Scale bars, 200 μm (B–E) and 10 μm (F–I).

overexpression of zebrafish caspase-3 induced apoptosis and served to modulate the pro-apoptotic signal during zebrafish development (Yabu et al., 2001). The expression level of *caspase-3* remained unchanged, or slightly reduced, in the *klf11b-MO*-injected embryos compared to that in *Con-MO*-injected embryos (Figs. 4E and 4F). Northern blot analysis confirmed increased expression levels of *p53* and *bax*, as well as unchanged expression levels of *caspase-3*, in the *klf11b-MO*-injected embryos (Fig. 4G). These findings suggested that the phenotype of *Klf11b* knockdown embryos might be rescued by reduced expression of *p53*. To test this, we performed the TUNEL assay in *klf11b-MO*- and/or *p53-MO*-injected embryos at 26 hpf (Figs. 4H–4K). Apoptotic cells were observed in embryos injected with *Con-MO* (Fig. 4H, n=50), as well as in embryos injected with *klf11b-MO* (Fig. 4I, n=23). However, the number of apoptotic cells was dramatically reduced in embryos co-injected with *klf11b-MO* and *p53-MO* (Fig. 4K, n=34), as well as in embryos injected with *p53-MO* (Fig. 4J, n=29). MO-mediated knockdown of *p53* in *klf11b-MO*-injected embryos rescued the apoptotic phenotype, implying that the function of Klf11b was equivalent to that of p53 or was upstream of

https://doi.org/10.12717/DR.2022.26.2.79

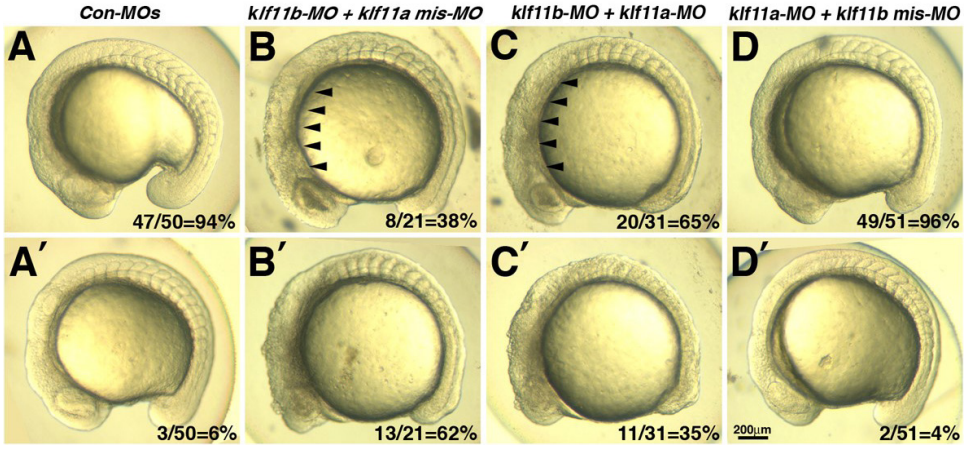

Fig. 3. Phenotypic analysis of *klf11a* and *klf11b* morphants. Lateral views, anterior to the left. The mixture of *klf11a mismatch-MO* and *klf11b mismatch-MO* (*Con-MOs*) was injected into zebrafish eggs as a control (A and A', n=50). At the 15-somite stage, degenerative and developmental defects (arrowheads) are observed in embryos injected with *klf11b-MO* and *klf11a mismatch-MO* (B and B', n=21), as well as in embryos injected with *klf11b-MO* and *klf11a-MO* (C and C', n=31), but not in embryos injected with *klf11a-MO* and *klf11b mismatch-MO* (D and D', n=51). Scale bars, 200 μm. MO, morpholino.

p53 in the *p53*-dependent apoptotic pathway.

3. Zebrafish *klf11b* morphant reduces the number of proliferative cells

To determine which cell types are most strongly affected after knockdown of *klf11b* function, *Tg[islet1-GFP]* embryos were injected with *klf11b-MO*, and then labeled with an antibody that recognized phosphorylated histone H3 on Ser-10 (PH3), an established marker for chromosome condensation during mitosis (Fig. 5, Hendzel et al., 1997; Higashijima et al., 2000). In the *Tg[islet1-GFP]* line, *GFP* mRNA is expressed in a majority of cranial motor neurons, in a manner similar to that of *islet-1* mRNA, beginning at 21 hpf (Higashijima et al., 2000). At 36 hpf, GFP-positive cranial motor neurons were well organized spatiotemporally in the central nervous system (CNS) of *Con-MO*-injected embryos (Fig. 5A), whereas morphological and spatial disorganization of GFP-positive cells was observed in the CNS of *klf11b-MO*-injected embryos (Fig. 5D). Although the number of GFP-positive cells was difficult to determine, the number of PH3-positive cells significantly decreased in *klf11b-MO*-injected embryos (Fig. 5E; 122.3±9.3, n=6), compared to that in the *Con-MO*-injected embryos (Fig. 5B; 342.8±8.7, n=4). These observations implied that reduction of proliferating precursors may be caused by apoptosis.

DISCUSSION

We identified and characterized zebrafish *Klf11b* as a homolog of human KLF10. Structural comparisons showed that zebrafish Klf11 homologs are highly conserved, with respect to human KLF10 and KLF11. Both zebrafish *klf11a* and *klf11b* mRNA are maternally expressed. During zebrafish development, *klf11a* is expressed in the ventral telencephalon and anterior lateral line, while *klf11b* is highly expressed in the olfactory blub, lens, PNDs, lateral primordia, and somites. However, only *klf11b* transcripts can be detected at the gastrulation stage. This might be the cause of epiboly retardation in *klf11b* morphants, as well as the source of their degenerative phenotype after this stage. Although structural preservation of zebrafish Klf11 homologs strongly suggests

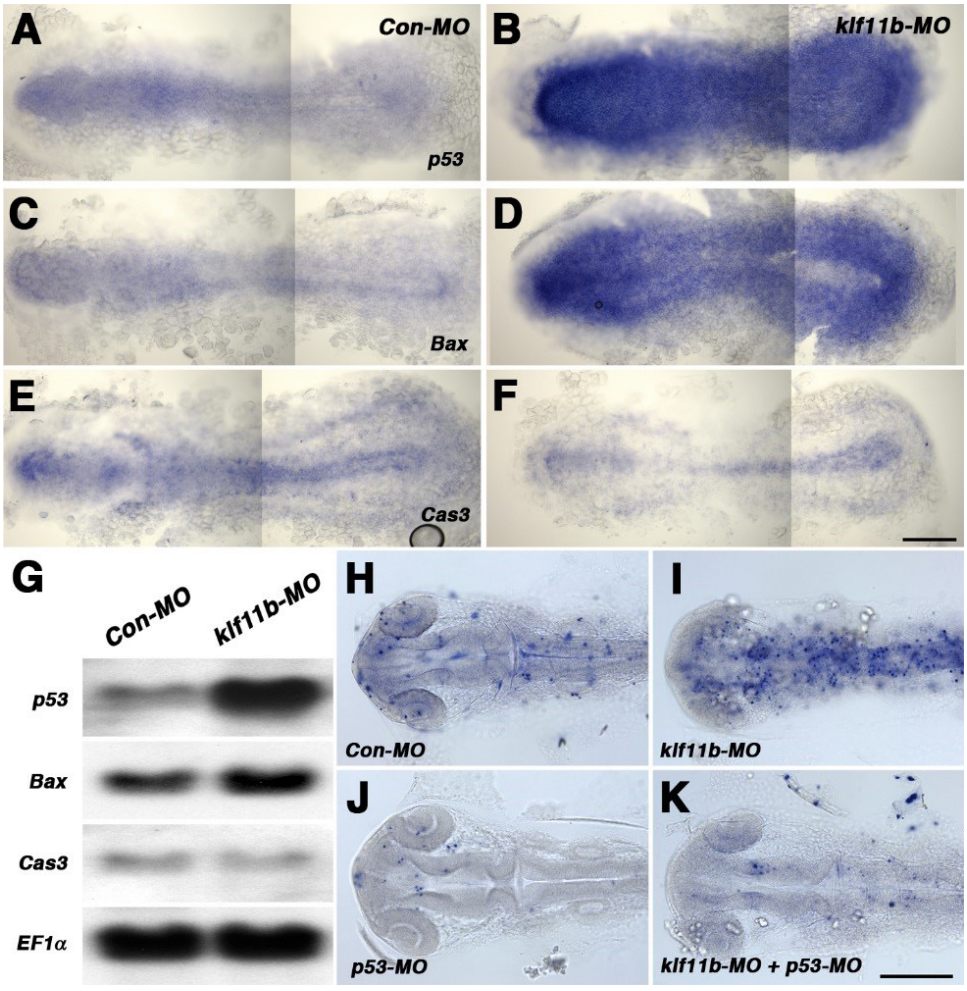

Fig. 4. Cell death in zebrafish *klf11b* morphants. Dorsal view (A–F, H–K), anterior to the left. Whole-mount *in situ* hybridization shows expression of *p53* (A, B), *Bax* (C, D), and *Cas3* (E, F) in the *klf11b mismatch-MO*-(*Con-MO*) (A, C, E) and *klf11b-MO*-injected embryos (B, D, F) at the 5-somite stage. (G), Northern blot analysis of zebrafish *p53*, *Bax*, *Cas3*, and *EF1α* mRNA. In total, 20 μg of total RNA from *Con-MO*-injected embryos and *klf11b-MO* injected embryos are applied to each lane. (H–K), TUNEL assay was performed on *Con-MO*-(H), *klf11b-MO*-(I), *p53-MO*-(J), and a mixture of *klf11b-MO*- and *p53-MO*-injected embryos (K) at 28 hpf. Apoptotic cells (blue dots) are observed in embryos injected with *klf11b-MO* (I, n=23), as well as those injected with *Con-MO* (H, n=50), but small numbers in embryos injected with *p53-MO* (J, n=29) or co-injected with *klf11b-MO* and *Con-MO* (K, n=34). Scale bars, 200 μm (A–F, H–K). MO, morpholino.

conservation of KLF homolog functions during evolution, the function and expression according to specific spatiotemporal patterns may have varied among individual subtypes.

Structural alignment showed that three zinc-finger domains of human KLF10 had approximately 79% and 84% similarity to zebrafish *Klf11a* and *Klf11b*, respectively, whereas human KLF11 had approximately 88% and 93% similarity to zebrafish *Klf11a* and *Klf11b*, respectively. Although zebrafish *Klf11b* is classified as a homolog of human KLF10 based on comparison of the overall AA sequence, zinc-finger domains of zebrafish Klf11b showed greater similarity with those of human KLF11. This may be why zebrafish *Klf11a* and *Klf11b* were characterized as human KLF11 homologs. In the zebrafish genome assembly, another Klf homolog is present: Klf10, in chromosome 16. Human KLF10 and zebrafish Klf11b consist of 469 and 458 AAs, respectively, whereas zebrafish Klf10 only contains 218 AAs. Comparison of predicted AA sequences showed

https://doi.org/10.12717/DR.2022.26.2.79

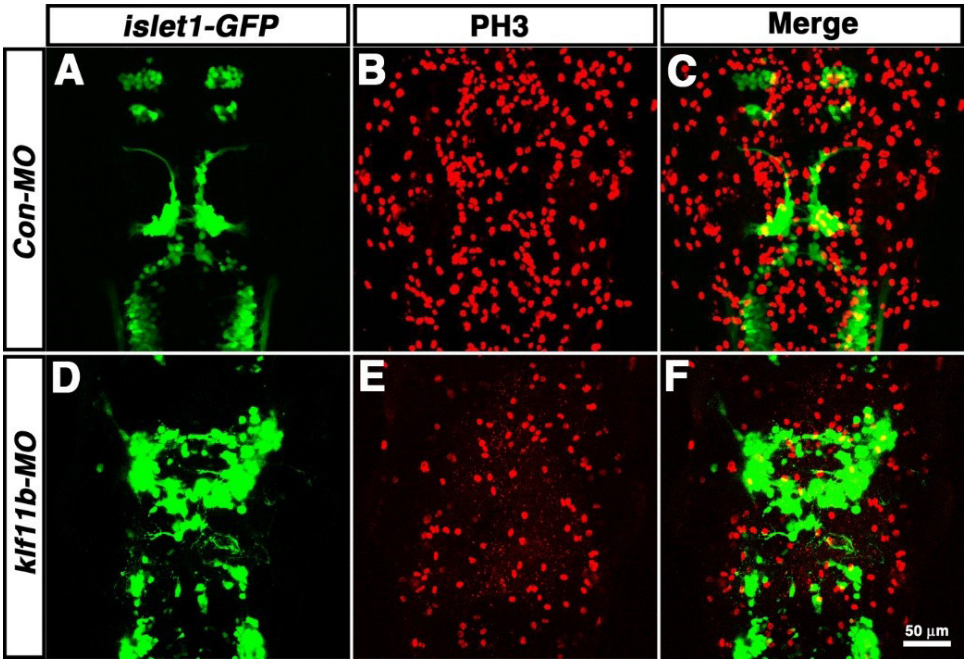

Fig. 5. KLF10 negatively regulates p53 activity as well as transcription of *p53*. (A), Human KLF10 (hKLF10) abolish activity of the human p53 promoter in transiently transfected HEK 293 cells (mean±SD, n=3 independent transfections, * p<0.01). HEK 293 cells were co-transfected with p53-Luc reporter (2 μg) and increasing amounts of myc-hKLF10 (0, 0.5, 1, and 2 μg) plasmid DNAs. (B), Human KLF10 modulates p53-dependent transcription. HEK 293 cells were co-transfected with PG13-Luc reporter (2 μg) and increasing amounts of myc-hKLF10 (0, 0.5, 1, and 2 μg) plasmid DNAs (mean±SD, n=3, ** p<0.01). Lower panel, Western blot analysis of myc-hKLF10, p53 and alpha-acetylated Tubulin (αTb) were performed to determine dose dependency of myc-hKLF10 in HEK 293 cells. (C), Upper panel, endogenous p53 interacts with hKLF10. HEK 293 cells transfected with Myc epitope-tagged full-length hKLF10 were subjected to immunoprecipitation (IP) with anti-Myc antibody. The immunocomplexes were analyzed by Western blot analysis with antibodies against p53 and Myc tag. Lower panel, pulldown assay of [^{35}S] methionine-labeled p53 ([^{35}S]Met-p53) were performed as described in materials and methods, by using purified GST and GST-hKLF10 fusion proteins. (D), Interaction between p53 and hKLF10 in the mammalian two-hybrid assay. The luciferase reporter pG5-Luc was co-transfected with the pairs of VP16-hKLF10 and p53-Gal4 into HEK 293 cells (1 μg of each). The experiment was repeated with a similar result (mean±SD, n=3, *** p<0.01). KLF, Krüppel-like factors.

that the zinc-finger domain (approximately 132 AAs) of zebrafish Klf10 had approximately 69%, 71%, 68%, and 68% similarity to zebrafish Klf11a, zebrafish Klf11b, human KLF10, and human KLF11, respectively. However, neither whole-mount *in situ* hybridization nor RT-PCR could detect zebrafish Klf10 transcripts (data not shown), suggesting that zebrafish Klf10 might be a pseudogene.

Northern blot analysis has shown that human KLF10 (TIEG1) transcripts are highly expressed in skeletal muscle, and moderately expressed in heart, placenta, and pancreas, whereas KLF11 (TIEG2) mRNA is ubiquitously expressed, with the highest levels occurring in the pancreas and skeletal muscle (Subramaniam et al., 1995; Cook et al., 1998). Human KLF11 is more prominently expressed in the pancreas, whereas KLF10 is expressed at higher relative levels in skeletal muscle (Cook et al., 1998). In zebrafish, whole-mount *in situ* hybridization showed that only *klf11b* transcripts are present in muscle, although both *klf11a* and *klf11b* are highly expressed in the brain of 3-day-old embryos. Taken together with the AA sequence comparison, the most likely classification of zebrafish *Klf11b* is as a homolog of human KLF10.

In the present study, we showed that a reduction in the number of proliferative precursor cells may be the result of cell death in zebrafish *Klf11b* morphants, suggesting that such cell death may

be mediated by p53. Biochemical analysis might elucidate that a KLF gene might be a negative regulator of *p53* transcription. Based on these observations, we propose three models: first, zebrafish Klf11b may function as a transcriptional repressor, with or without a corepressor, by binding to Sp1 elements of the *p53* gene; second, zebrafish Klf11b may function as a corepressor by binding to p53 protein; and finally, DNA-binding Klf11b may mask the function of p53 as a transcriptional activator. Although interaction of the corepressor mSin3A with an alpha-helical motif of Klf11/Klf10 supports one of our hypotheses (Zhang et al., 2001), previous studies have shown that overexpression of human KLF10 in cancer cell lines induced apoptosis, in a manner similar to that of the mitochondrial pathway (Tachibana et al., 1997; Ribeiro et al., 1999). Additionally, transgenic overexpression of KLF11 has been shown to result in a decreased number of proliferative cells, increased rate of apoptosis, and reduction in the size of the pancreas (Fernandez-Zapico et al., 2003). In human leukemia cells, overexpression of human KLF10 promoted chemically induced apoptosis through the mitochondrial pathway, as represented by upregulation of Bax, downregulation of Bcl-2, release of cytochrome C, and activation of caspase-3 (Jin et al., 2007). These studies indicate that loss of KLF10 function could promote carcinogenesis (Tachibana et al., 1997; Ribeiro et al., 1999; Fernandez-Zapico et al., 2003). Previous study provides some support for this hypothesis, based on treatment with carcinogens such as DMBA and TPA (Song et al., 2012). However, KLF10-deficient mice demonstrated increased numbers of apoptotic cells in DMBA/TPA-treated epidermis, and lower incidence of tumors, than wild-type mice, following DEN-induced liver tumorigenesis (Song et al., 2012; Heo et al., 2015).

Although human KLF6 is essential for hepatic carcinoma cells to evade p53-mediated apoptosis *in vitro* (Sirach et al., 2007), our study provides the first observation concerning the relationship between KLFs and p53 *in vivo*. To better understand the function of KLFs, further studies are needed to address their roles in apoptosis, as well as in tumorigenesis. First, KLF10 and KLF11 double KO mice could help determine the functions of these proteins. In humans, KLF10 and KLF11 exhibit approximately 84% similarity, and their expression pattern is very similar in adult human tissues (Cook et al., 1998). Based on the principal of genetic redundancy, KLF10 and KLF11 double KO mice may show functions of KLFs during gastrulation, as the expression of mouse KLF11 is unclear during early embryonic development. As described above, zebrafish *klf11b* is expressed at the gastrulation stage, whereas *klf11a* is not, and the apoptotic phenotype is observed after gastrulation. Second, co-immunoprecipitation with the KLF11b and p53 antibody as well as isolation and characterization of genes downstream of the KLF11b/p53 complex could aid in characterizing their functions. Finally, examination of p53 stability in the absence of mammalian KLF10 could help determine its function. Mungamuri and colleagues reported that USP7 deubiquitinase protected SUV39H1 from MDM2-mediated ubiquitination in the absence of a p53 stimulus (Mungamuri et al., 2016).

In summary, we have shown that *Klf11b* morphants undergo apoptosis, which may be mediated by p53. Zebrafish *Klf11b* morphants could be used in genetic screening for identification of unknown genes, as well as for identification of small molecules involved in chemically induced cell death. This model will greatly facilitate understanding of the homeostasis underlying cell viability, which is mediated by the interaction between KLF and p53.

REFERENCES

Black AR, Black JD, Azizkhan-Clifford J (2001) Sp1 and krüppel-like factor family of transcription factors in cell growth regulation and cancer. J Cell Physiol 188:143-160.

https://doi.org/10.12717/DR.2022.26.2.79

Cook T, Gebelein B, Mesa K, Mladek A, Urrutia R (1998) Molecular cloning and characterization of TIEG2 reveals a new subfamily of transforming growth factor-β-inducible Sp1-like zinc finger-encoding genes involved in the regulation of cell growth. J Biol Chem 273:25929-25936.

Fernandez-Zapico ME, Mladek A, Ellenrieder V, Folch-Puy E, Miller L, Urrutia R (2003) An mSin3A interaction domain links the transcriptional activity of KLF11 with its role in growth regulation. EMBO J 22:4748-4758.

Hendzel MJ, Wei Y, Mancini MA, Van Hooser A, Ranalli T, Brinkley BR, Bazett-Jones DP, Allis CD (1997) Mitosis-specific phosphorylation of histone H3 initiates primarily within pericentromeric heterochromatin during G2 and spreads in an ordered fashion coincident with mitotic chromosome condensation. Chromosoma 106:348-360.

Heo SH, Jeong ES, Lee KS, Seo JH, Lee WK, Choi YK (2015) Krüppel-like factor 10 null mice exhibit lower tumor incidence and suppressed cellular proliferation activity following chemically induced liver tumorigenesis. Oncol Rep 33:2037-2044.

Higashijima S, Hotta Y, Okamoto H (2000) Visualization of cranial motor neurons in live transgenic zebrafish expressing green fluorescent protein under the control of the *islet-1* promoter/enhancer. J Neurosci 20:206-218.

Jin W, Di G, Li J, Chen Y, Li W, Wu J, Cheng T, Yao M, Shao Z (2007) TIEG1 induces apoptosis through mitochondrial apoptotic pathway and promotes apoptosis induced by homoharringtonine and velcade. FEBS Lett 581:3826-3832.

Jung SH, Kim HS, Ryu JH, Gwak JW, Bae YK, Kim CH, Yeo SY (2012) Her4-positive population in the tectum opticum is proliferating neural precursors in the adult zebrafish brain. Mol Cells 33:627-632.

Kimmel CB, Ballard WW, Kimmel SR, Ullmann B, Schilling TF (1995) Stages of embryonic development of the zebrafish. Dev Dyn 203:253-310.

Mungamuri SK, Qiao RF, Yao S, Manfredi JJ, Gu W, Aaronson SA (2016) USP7 enforces heterochromatinization of p53 target promoters by protecting SUV39H1 from MDM2-mediated degradation. Cell Rep 14:2528-2537.

Oltval ZN, Milliman CL, Korsmeyer SJ (1993) Bcl-2 heterodimerizes in vivo with a conserved homolog, Bax, that accelerates programmed cell death. Cell 74:609-619.

Ribeiro A, Bronk SF, Roberts PJ, Urrutia R, Gores GJ (1999) The transforming growth factor β1–inducible transcription factor, TIEG1, mediates apoptosis through oxidative stress. Hepatology 30:1490-1497.

Sirach E, Bureau C, Péron JM, Pradayrol L, Vinel JP, Buscail L, Cordelier P (2007) KLF6 transcription factor protects hepatocellular carcinoma-derived cells from apoptosis. Cell Death Differ 14:1202-1210.

Song KD, Kim DJ, Lee JE, Yun CH, Lee WK (2012) KLF10, transforming growth factor-β-inducible early gene 1, acts as a tumor suppressor. Biochem Biophys Res Commun 419:388-394.

Subramaniam M, Harris SA, Oursler MJ, Rasmussen K, Riggs BL, Spelsberg TC (1995) Identification of a novel TGF-β-regulated gene encoding a putative zinc finger protein in human osteoblasts. Nucleic Acids Res 23:4907-4912.

Subramaniam M, Hawse JR, Rajamannan NM, Ingle JN, Spelsberg TC (2010) Functional role of KLF10 in multiple disease processes. Biofactors 36:8-18.

Tachibana I, Imoto M, Adjei PN, Gores GJ, Subramaniam M, Spelsberg TC, Urrutia R (1997) Overexpression of the TGFbeta-regulated zinc finger encoding gene, TIEG, induces apoptosis in pancreatic epithelial cells. J Clin Invest 99:2365-2374.

Xue Y, Gao S, Liu F (2015) Genome-wide analysis of the zebrafish Klf family identifies two genes important for erythroid maturation. Dev Biol 403:115-127.

Yabu T, Kishi S, Okazaki T, Yamashita M (2001) Characterization of zebrafish caspase-3 and induction of apoptosis through ceramide generation in fish fathead minnow tailbud cells and zebrafish embryo. Biochem J 360:39-47.

Yeo SY, Miyashita T, Fricke C, Little MH, Yamada T, Kuwada JY, Huh TL, Chien CB, Okamoto H (2004) Involvement of Islet-2 in the Slit signaling for axonal branching and defasciculation of the sensory neurons in embryonic zebrafish. Mech Dev 121:315-324.

Zhang JS, Moncrieffe MC, Kaczynski J, Ellenrieder V, Prendergast FG, Urrutia R (2001) A conserved α-helical motif mediates the interaction of Sp1-like transcriptional repressors with the corepressor mSin3A. Mol Cell Biol 21:5041-5049.

https://doi.org/10.12717/DR.2022.26.2.79